An Explainable Classification Framework for Determining and Understanding the Suitability of Solvent Extraction for Bioproduct Recovery

Jianping Li[ac], Reid C. Van Lehn[ac], Christos T. Maravelias[b*]

[a] *Department of Chemical and Biological Engineering, University of Wisconsin-Madison, Madison, WI 53706, United States*

[b] *Department of Chemical and Biological Engineering and Andlinger Center for Energy and the Environment, Princeton University, Princeton, NJ 08540, United States*

[c] *DOE Great Lakes Bioenergy Research Center, Madison, WI 53726, United States*

*Email: maravelias@princeton.edu

Abstract

Lignocellulosic biomass is an abundant feedstock for producing sustainable fuels and chemicals. However, a key challenge in most biomass utilization strategies is the recovery of products from a dilute, typically aqueous, phase. In this respect, liquid-liquid extraction, which relies on a solvent to transfer a product of interest from one liquid phase to another (solvent-rich) phase, is a technology that can reduce energy requirements for product recovery. To reduce solvent consumption, liquid-liquid extraction needs to be combined with another separation method (e.g., distillation) to recycle the solvent. Despite the research on solvent extraction, there are limited system-wide methods that allow us to determine when extraction is well suited to carry out a specific separation. Accordingly, we present a classification framework to predict if extraction, coupled with distillation, is feasible and more economical than distillation. Our framework is based on features such as feed composition, liquid-liquid equilibrium constants, relative volatilities, and solvent price, and leads to trained classifiers that show good prediction accuracy. We further study how specific features influence the suitability of extraction and, to showcase the applicability of the framework, we use it to analyze the separation of acetic acid from water.

Key words: Separation, Extraction, Distillation, Optimization, Explainable Classification

1. Introduction

Lignocellulosic biomass is an abundant and sustainable feedstock[1] that can be used to produce more than thirty biomass-derived chemicals (referred to as "bioproducts" hereafter).[2] The production of such bioproducts can potentially improve the economic viability of biorefineries while replacing other more emission-intensive processes.[3] However, these bioproducts have to be often recovered from dilute streams (bioreactor effluents), which means that their recovery can be energy intensive.[4] Hence, given that separation processes can account for up to 40%–60% of the total energy consumed in chemical processes,[5] employing efficient separation methods is necessary to keep the energy requirements and environmental impact of the biorefinery low.[6] These motivate research into determining the feasibility of a separation method and understanding the selection of energy-efficient separation methods among many alternatives. Distillation and liquid-liquid extraction are two common separation methods.[7-9]

Distillation uses differences in volatilities between mixture components to drive separation.[6] The distillation of feed streams with low-concentration products often requires high energy consumption[10, 11] which can be reduced through heat integration[12], heat pumps[13], and process intensification (e.g., reactive distillation and extractive distillation).[14-16]

Liquid-liquid extraction uses differences in the partitioning of mixture components between two immiscible liquid phases[17] which are formed by adding an immiscible solvent to a homogenous mixture that initially contains the product to drive separation. These two phases are the solvent-rich and the solvent-lean phases. Liquid-liquid extraction is a promising technology for the recovery of bioproducts because they are often produced at low-concentrations.[18] For example, the concentration of 2-pyrone-4,6-dicarboxylic acid (PDC) in the outlet stream from the microbial conversion of lignin was identified to be at most 0.15 mM.[19] In liquid-liquid extraction, components are classified as the product, the diluent (carrier of product in the feed stream), and the solvent. Product partitioning from the solvent-lean phase into the solvent-rich phase occurs due to the product's higher thermodynamic affinity for the solvent than the diluent. When an appropriate solvent system is identified, liquid-liquid extraction allows:[6] (1) high partitioning of the product into the solvent-rich phase, (2) easy separation of the product from the solvent, (3) low partitioning of the solvent into the solvent-lean phase to minimize solvent loss, and (4) low partitioning of water into the solvent-rich phase; while also achieving low solvent toxicity and low solvent price. More efficient partitioning of a product into the solvent-rich phase can be achieved via multi-stage countercurrent liquid-liquid extraction.[20]

To recycle the solvent and further purify the product, liquid-liquid extraction is often followed by distillation, which results in a separation system commonly referred to as hybrid extraction and distillation.[21-23] In this case, a large volatility difference between the solvent and the product facilitates easy separation between them. For brevity, we refer to hybrid extraction and distillation as "extraction" (since liquid-liquid extraction is the first separation method); and refer to a standalone distillation as "distillation". While extraction has been suggested for the recovery of products from various mixtures (e.g., butanol separation from acetone–butanol–ethanol fermentation mixtures[22] and furfural recovery from aqueous methanol–acetic acid–furfural mixtures[24]), it remains unclear under what conditions extraction is a competitive technology.[13] To address this question, Scheffczyk et al. developed a framework for the integrated design of molecules and separation processes using short-cut pinch-based liquid-liquid extraction and distillation models;[25] and Blahušiak et al. reviewed short-cut calculations to decide among the use of distillation, liquid-liquid extraction, extractive distillation, and heat pump-assisted distillation.[26] However, these prior studies have not considered the operating costs due to solvent consumption and the trade-offs between operating and capital costs. Moreover, the influence of several features (e.g., feed composition, liquid-liquid equilibrium constants, relative volatilities, and solvent price) on the selection of separation methods has not been elucidated, and there are no predictive methods to identify when extraction is feasible and more economical than distillation. The fundamental questions that remain open are the following: (1) Under what conditions is extraction feasible (i.e., when the desired product purity and recovery can be achieved using extraction)? (2) Under what conditions is extraction more economical than distillation? (3) How do process parameters influence extraction feasibility and the selection between extraction and distillation? We define extraction suitability in terms of two aspects: (1) the extraction feasibility, and (2) the selection between extraction and distillation.

We develop an explainable classification framework to predict labels (i.e., if extraction is feasible and more economical than distillation) based on features such as feed composition, liquid-liquid equilibrium constants, relative volatilities, and solvent price. We first define a space of feature values by predicting relevant thermodynamic property ranges. We model liquid-liquid extraction using a stage-by-stage model[20] and distillation using a short-cut model.[7, 27] These models are solved for given input feature values with cost minimization as the objective function. Then, we train binary classification models (classifiers) using a subset of feature values to predict labels. Furthermore, calculating Shapley values based on the trained classifiers allows us to

identify which features are important and, thereby, better understand when extraction can be a competitive technology. This article is structured as follows. First, we provide background. Then, we present the explainable classification framework. Next, we apply the proposed framework to identify the key classifier features for the selection between extraction and distillation to achieve the separation of bioproduct from aqueous phase using various solvents. Finally, we identify separation methods for separating acetic acid from water.

2. Background

In this section, we first give the problem statement, then discuss the basics concepts in liquid-liquid extraction and distillation, and close with an introduction of the used data analysis methods.

2.1. Problem Statement

We focus on the separation of aqueous streams that contain bioproducts in low concentrations.[4] Using distillation to recover bioproducts from such streams is energy intensive, which makes the identification of other separation methods critical for biomass valorization.[28] To simplify the discussion, we assume that the feed stream only contains water and one product. For a standalone liquid-liquid extraction, we consider a ternary system of product (P), water (W), and solvent (S). The diluent is water, and the solvent-lean phase is the aqueous (AQ) phase. Nevertheless, the analysis we present can be extended to separations of other mixtures if the desired separation can be achieved using the extraction structures discussed in Figure 2 and the feature values are within the ranges investigated in this work (Table 1).

Given are (1) feed stream specification (i.e., product mole fraction); (2) product stream specifications (i.e., product recovery and purity); (3) physical properties (liquid-liquid equilibrium constants, relative volatilities); (4) capital and operational cost coefficients for distillation and extraction, including solvent price; and (5) the maximum number of liquid-liquid extraction stages. Based on these specifications, we determine other parameters using the calculation methods described in Section S5 of the Supporting Information. We consider the following features: liquid-liquid equilibrium constants, relative volatilities, solvent price, and product mole fraction in feed. The above features influence the feasibility and cost of extraction, while relative volatilities and the product mole fraction in feed influence the cost of distillation.

2.2. Liquid-liquid Extraction and Distillation

Figure 1 illustrates standalone liquid-liquid extraction (Figure 1A) and distillation (Figure 1B)

units. For the standalone liquid-liquid extraction (denoted as EXT in Figure 1A) column, the feed stream of water-product mixture and a solvent stream enters at the first stage and the last stage of the EXT column, respectively. The product partitions from the aqueous (AQ) phase into the solvent-rich (SO) phase. The outlet streams are the (solvent-rich) extract and (aqueous) raffinate. We consider isothermal liquid-liquid extraction.

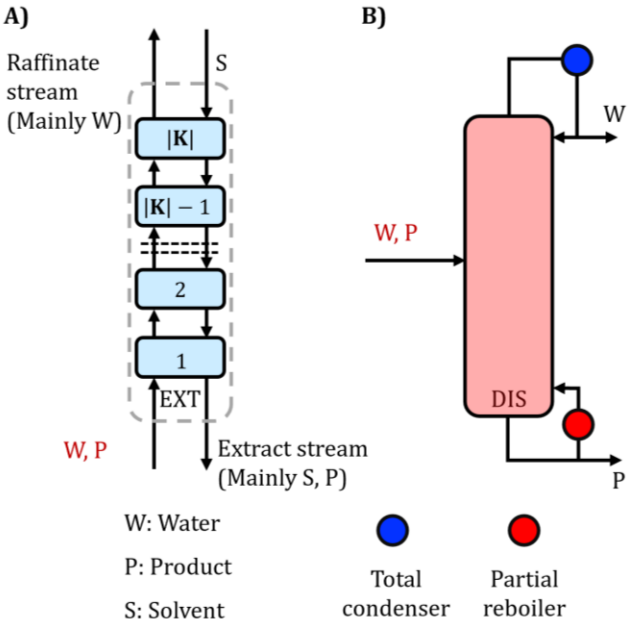

Figure 1. Illustration of separation methods. A) standalone liquid-liquid extraction. B) standalone distillation.

The critical physical properties for the EXT are equilibrium constants. We consider ternary systems where the product mole fraction is low such that equilibrium constants are composition-independent and identical at all extraction stages.[20] We use $k \in \mathbf{K}$ to denote stages in EXT column and define liquid-liquid equilibrium constant, κ_j, for component $j \in \mathbf{J}$ as follows:

$$\kappa_j = \frac{X_{j,k}^{SO}}{X_{j,k}^{AQ}}, \forall\ j \in \mathbf{J}, k \in \mathbf{K} \tag{1}$$

where $X_{j,k}^{SO}$ is the mole fraction of component j at stage k in the solvent-rich phase and $X_{j,k}^{AQ}$ is the mole fraction of component j at stage k in the aqueous phase. If a ternary system has composition-dependent κ_j, then we use the average of equilibrium constants within the column. The details of this averaging procedure are given in Section S3 of Supporting Information.

The same water-product mixture stream can also be fed into a standalone distillation

(denoted as DIS in Figure 1B) column. Since most products have higher boiling points than water [2], the product is withdrawn from the bottom of DIS while the water is withdrawn from the top. We consider distillation of near-ideal mixtures, allowing us to assume constant volatility. The critical physical property for DIS is the relative volatility of a component j with respect to a reference component j':

$$\alpha_{j,j'} = \frac{K_j}{K_{j'}} = \frac{y_j/x_j}{y_{j'}/x_{j'}}, \forall\, j \in \mathbf{J} \tag{2}$$

where K_j is the ratio of the vapor mole fraction (y_j) to the liquid mole fraction (x_j). The reference component is often chosen as the heaviest component (HC) so that all $\alpha_{j,j'} > 1$. Although $\alpha_{j,j'}$ is defined based on the HC when modeling DIS, it is converted to $\alpha_{j,j'}$ with the product as the reference component when training classifiers, and thus can be greater than or smaller than 1.

2.3. Data Analysis Methods

In this section, we discuss concepts of classification, Shapley values, and feature elimination.

Binary Classifiers. A classification model (classifier) relates the values of a set of input features (feature vector) to a label. We study binary classifiers in which feature vectors are labeled with one of two possible classes. To train a binary classifier, a data set consisting of multiple feature vectors and associated labels is defined; each feature vector-label combination is referred to as a sample. A classifier is trained by choosing a subset of samples (training set) from the full data set and using these samples to determine classifier parameters as discussed further below. The classifier's accuracy is quantified by predicting labels for a subset of samples not used during model training (test set) and comparing predicted labels to the known labels. Once trained, the classifier can predict labels for new feature vectors. In this work, we train two different types of binary classifiers: (1) an extraction feasibility classifier to predict whether extraction is feasible, and (2) a separation selection classifier to predict whether extraction is selected over distillation.

Random Forest Classifier. A random forest (RF) is a combination of tree predictors. Each tree independently and randomly samples from the training set and further introduces random attribute selection during the training process.[29] The final prediction is determined by the majority predictions from all tree predictors. Classification based on RF is computationally fast but does not yield an explicit expression. We implemented RF using Scikit-learn 1.0.1.[30]

Support Vector Machine. A support vector machine (SVM) yields a boundary between two

classes by maximizing the distance between points in the two classes.[31, 32] Prediction of a given feature vector $\boldsymbol{\lambda^G}$ using the trained SVM can be evaluated as follows:

$$\text{Prediction} = \begin{cases} 0 \quad if \quad \sum_{s=1}^{|S|} \delta_s^* \mu_s K(\boldsymbol{\lambda_s}, \boldsymbol{\lambda^G}) + \varepsilon^* < 0 \\ 1 \quad if \quad \sum_{s=1}^{|S|} \delta_s^* \mu_s K(\boldsymbol{\lambda_s}, \boldsymbol{\lambda^G}) + \varepsilon^* \geq 0 \end{cases} \tag{3}$$

where, $\boldsymbol{\lambda_s}$ is the feature vector for sample $s \in S$; μ_s is the label of sample s; δ_s^* and ε^* are dual coefficient for sample *s* and intercept coefficient for trained SVM, respectively;[33] and $K(\boldsymbol{\lambda_s}, \boldsymbol{\lambda^G})$ is the kernel function. We implemented SVM using Scikit-learn 1.0.1 with $K(\boldsymbol{\lambda_s}, \boldsymbol{\lambda^G}) = \exp(-\gamma^{SVM} \|\boldsymbol{\lambda_s} - \boldsymbol{\lambda^G}\|^2)$,[30] where γ^{SVM} is a hyperparameter.

Shapley Values for Interpreting the Prediction of Classifiers. To explain the influence of feature values on the prediction of classifiers, we determine Shapley values for all features and for each sample. A Shapley value in cooperative game theory informs how a player contributes to the result of a game.[34] When applied to machine learning (ML) models, the cooperative game can be defined such that features are "players" that interact to determine model predictions.[35] Hence, Shapley values can be used to interpret the contribution of each feature to model predictions for a particular set of feature values (*i.e.*, a particular feature vector). The importance of a feature, in general, can be determined by averaging the absolute Shapley values per feature across the full training set.[36] Shapley values can be computed for any predictive models and are suitable for nonlinear data sets. We calculated Shapley values using the Shapley Additive Explanations (SHAP) method with TreeExplainer.[37] In addition to a single feature's Shapley value, the SHAP method can also compute Shapley values for pairwise feature interactions to quantify the influence of feature pairs on model predictions. The SHAP value computation for RF is faster than that for SVM. Hence, when generating design guidelines, we use the RF classifier (Section 4.2). When explicit expressions are needed, we use SVM (Section 4.5).

Prediction Accuracy. Classifier prediction accuracy is defined as the ratio of correctly classified samples within the test set, and it is determined using the accuracy score of Scikit-learn 1.0.1.[30]

Feature Elimination. To simplify the discussion of how specific features influence the predictions of classifier, we reduced the complete set of features by identifying only those that substantially influence prediction accuracy. To achieve this, we implemented a recursive feature

elimination procedure: starting with all features, we trained a classifier iteratively with the least important feature (based upon the feature importance implied by the SHAP values) eliminated from the input feature vectors. This procedure terminated once a significant reduction in the classifier's prediction accuracy was observed. The remaining features are defined as the key features that will be studied using the explainable classification framework described below.

3. Explainable Classification Framework

In this section, we develop an explainable classification framework (Figure 2) for determining and understanding the extraction suitability, which involves: (1) prediction of a physically relevant space of thermodynamic properties; (2) generation of feature values by sampling within the identified space of thermodynamic properties and other feature ranges; (3) separation modeling; (4) identification if extraction is feasible and calculation of the costs of extraction and distillation systems; (5) training of classifiers to predict the extraction suitability; and (6) interpretation of classifier predictions to generate design guidelines.

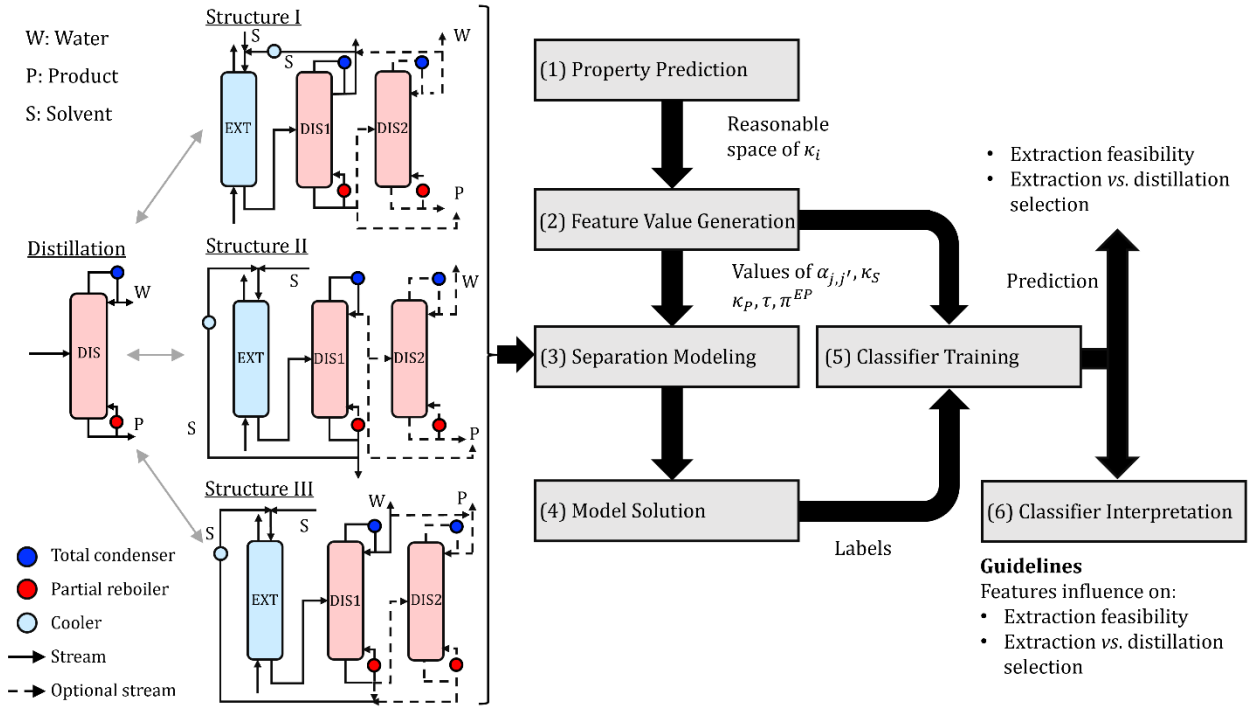

Figure 2. Explainable classification framework. Representative extraction structures include structure I for mixtures with $\alpha_{W,P}, \alpha_{S,P} > 1$, and structure II and structure III for mixtures with $\alpha_{W,S} > \alpha_{P,S} > 1$. Solid lines indicate process streams always having positive flows. Dashed lines indicate optional streams. We consider the distillation column with a total condenser and a partial reboiler.

The details of property prediction [38, 39] are given in Section S2 of Supporting Information. For separation modeling, we consider and discuss three representative extraction structures based on the ranking of relative volatility (Section 3.2). The remainder of this section discusses generation of feature values, separation modeling, and the cost function for separation methods. Moreover, we describe the implementation of separation modeling, sampling, optimization, and classification.

3.1. Generation of Feature Values

The feature space is bounded within the space defined by the ranges given in Table 1. We bounded κ_W within [0.01, 0.02] to represent solvents that enable low water partitioning into the SO phase. To ensure that κ_j are physically reasonable, we further bounded values of κ_j within a three-dimensional convex hull constructed from values of κ_j for water, solvents, and representative products obtained using the property prediction methods. The details of this convex hull construction procedure are given in Section S3 of Supporting Information. We sampled feature values within the constructed convex hull and within the ranges of feature values in Table 1. Depending on the $\alpha_{j,j'}$ ranking, our sampling involves additional constraints (e.g., $\alpha_{S,P} > \alpha_{W,P}$). Note that during sampling, κ_j and $\alpha_{j,j'}$ are independent of each other.

Table 1. Features used in separation modeling and classification.

Features	Range
$\alpha_{j,j'}$ relative volatility between component *j* and component *j'*	[1.1, 2]
κ_S liquid-liquid equilibrium constant of solvent	[1, 1000]
κ_P liquid-liquid equilibrium constant of product	[1, 50]
τ product mole fraction in feed	[0.01, 0.1]
π^{EP} solvent price ($ per kmol solvent)	[50, 6000]

3.2. Separation Modeling

We model three representative extraction structures (Figure 2 Left) based on the predicted properties of commonly used solvents and products given in Section S4 of Supporting Information. The property prediction results indicate that of the 747 solvents modeled: (1) 14.2% are miscible with water, (2) 58.9% are immiscible with water and heavier than water, and

(3) 26.9% are immiscible with water and lighter than water. Moreover, all 37 products, except ethanol, are heavier than water. Solvents can be heavier or lighter than products. This analysis suggests three representative structures: (1) structure I for the case where the product is the heaviest and no restriction exists on the ranking of relative volatilities for solvent and water, (2) structure II for the case where $\alpha_{W,S} > \alpha_{P,S} > 1$ and the second potential distillation column separates P from W, and (3) structure III for the case where $\alpha_{W,S} > \alpha_{P,S} > 1$ and the second potential distillation column separates P from S. The specifications for all systems are (1) total product flowrate of 1 kmol/s, (2) 95% product purity, and (3) 90% product recovery.

Description of Separation Structures. In all extraction structures (Figure 2 Left), the product partitions into the SO phase coming out of EXT while most of the water from the feed remains in the raffinate stream. The extract stream from EXT is fed to DIS1 to separate the product from solvent and water. DIS2 can be further used to meet product purity and recovery requirements. The solvent recycle stream from DIS1 is cooled to 25°C and a purge stream is allowed to remove excessive water.

In structure I, if $\alpha_{S,P} > \alpha_{W,P}$, then solvent is mainly recycled to EXT from the top of DIS1. DIS2 mainly separates the product from water. In structure I, water is purged at the top of DIS2. If $\alpha_{W,P} > \alpha_{S,P}$, then solvent is recycled from the top of DIS1 and DIS2. DIS2 separates the product from solvent. In structure I, since water partitioning into the SO phase is low, the water flow in the top of DIS1 is also low. In structure II, solvent is recycled to EXT from the bottom of DIS1. If product purity and recovery requirements are met, the top outlet stream from DIS1 is withdrawn as product. Otherwise, this top stream flows into DIS2. In structure II, water and product are obtained at the top and the bottom of DIS2, respectively. In structure III, if product purity and recovery requirements are met, the top outlet stream from DIS1 is withdrawn as product and solvent is recycled to EXT from the bottom of DIS2. Otherwise, water is purged through the top stream of DIS1, while the bottom stream of DIS1 is fed into DIS2. In this case for structure III, solvent is recycled to EXT from the bottom of DIS2 and product is obtained at the top of DIS2.

Mathematical Model. We model EXT using a stage-by-stage model with constant $\boldsymbol{\kappa_j}$.[20] All distillation columns are modeled using the short-cut Underwood-Fenske model,[27] where we fix the total product flow rate ($\boldsymbol{\psi^B}$), product purity ($\boldsymbol{\omega}$), and product recovery ($\boldsymbol{\gamma}$). For the model of the standalone distillation, the product mole fraction in feed is fixed as $\boldsymbol{\tau}$. The key decision variables in the short-cut distillation model include the minimum number of stages, and the

minimum vapor flows in the rectifying and stripping section. Moreover, we determine the ranges of underwood roots based on the relative volatilities of the heavy (HK) and light key (LK) components (shown in Eqs. S35 – S37 of Supporting Information).

The criteria for the selection of the key components (Table 2) are as follows: (1) DIS1: HK and LK components are the heaviest and the lightest components, respectively; (2) DIS2: HK and LK components are adjacent to each other in terms of relative volatilities. The models include additional mole balances, stream connectivity constraints, as well as balances around mixers and splitters. We approximate the heat duty of coolers using the enthalpy change across the coolers and approximate the distillation operating cost based on the minimum vapor flow (shown in Section S5 of Supporting Information).

Table 2. Heavy (HK) and light key (LK) components for distillation.

Key components	structure I	structure II	structure III
HK in DIS1	P	S	S
LK in DIS1	W or S (not adjacent with P)	W	W
HK in DIS2	P	P	S
LK in DIS2	W or S (adjacent with P)	W	W

3.3. Cost Function

We seek to minimize the total annualized cost per kmol product, which consists of capital and operating costs. Cost parameters are obtained by fitting cost data generated using the Aspen Process Economic Analyzer to the proposed functional form (Eqs. S71 – S72 of Supporting Information). Model details, cost parameter determination, and model reformulations are given in Section S5 of Supporting Information.

3.4. Implementation

We sample feature values from the space introduced in Section 3.1 using Latin Hypercube sampling. These feature values are input to the systems models, described in the previous section and implemented in GAMS, to determine the label for each feature vector. The input feature values for structures II and III are the same since these structures are applicable to systems that have the same relative volatility ranking. The models are solved using the global optimization solver BARON,[40] using parallel computing resources.[41] A resource limit of 5 CPU hours and an

optimality tolerance of 1% for each model are used. For structure I, 50,000 and 2,000 samples are used as initial training and test sets, respectively. For structure II and III, 25,000 and 2,000 samples are used as initial training and test sets, respectively. For all extraction structures, the initial sets are mixed as a full data set and stratified sampling based on τ (product mole fraction in feed) is implemented, resulting in new training and test sets with a size identical to the initial training and test sets. This procedure improves the prediction accuracy of the six classifiers (extraction feasibility and separation selection classifiers for each of the three extraction structures). During feature elimination, this stratified sampling is not implemented since τ may not be a key feature. Cross validation for hyperparameter tuning is implemented to avoid overfitting. When training the RF classifier, we use the GridSearch method and 5-fold cross validation for hyperparameter tuning. GridSearch is implemented in Scikit-learn 1.0.1 with the following hyperparameters: (1) the maximum depth of the tree (max_depth), (2) the minimum number of samples required to split an internal node (min_samples_split), (3) the type of function to measure a split's quality (criterion), and (4) the minimum number of samples required to be at a leaf node (min_samples_leaf). When training the SVM, we use the MATLAB function fitcsvm with hyperparameter optimization, the standardize option, and 5-fold cross validation.[42]

4. Results and Discussion

In this section, we apply the proposed framework to investigate the influence of the key features on the extraction suitability. We then apply the framework for separating acetic acid from water.

4.1. Prediction Accuracy and Key Features of Classifiers

We use reduction of prediction accuracy during feature elimination to identify key features. Based on its definition in Section 2.3, without feature elimination, the prediction accuracy of the extraction feasibility classifiers is 0.98 for structure I, 0.98 for structure II, and 0.96 for Structure III. Similarly, without feature elimination, the prediction accuracy of the separation selection classifiers is 0.97 for structure I, 0.98 for structure II, and 0.96 for structure III.

The update of prediction accuracy for extraction feasibility and separation selection classifiers during feature elimination is given in Figure S6. The key features for the extraction feasibility classifiers are given in Section S6 of Supporting Information. For separation selection classifiers, removing κ_S reduces prediction accuracy significantly (i.e., from higher than 0.94 to lower than 0.87) for structure I. Hence, κ_S, π^{EP}, $\alpha_{W,P}$ are the key features of the separation

selection classifier for structure I. Similarly, removing κ_S significantly reduces prediction accuracy (i.e., from 0.94+ to less that than 0.86) for structure II and III. Hence, κ_S, π^{EP}, and $\alpha_{W,P}$ are key features of the classifiers for structure II and III. Moreover, based on the sample information in Section S6 of Supporting Information, we consider structure III as the major structure when $\alpha_{W,S} > \alpha_{P,S} > 1$.

4.2. Interpretation of Classifiers

Having established the prediction accuracy of the trained classifiers, we investigate the features' influence on the predictions of the classifiers by analyzing the SHAP values, which are given in Figure S7 for the extraction feasibility classifier and Figure 3 for the separation selection classifier. We discuss the extraction feasibility classifier in Section S6 of Supporting Information.

The Summary plot of Figure 3 indicates the influence of the key features on the selection between extraction and distillation. Features are listed along the y-axis of the Summary plots from top to bottom in order of decreasing importance. Each point in the Summary plot corresponds to a single feature value for a specific sample (*i.e.*, a feature vector with the corresponding label). In Figure 3, each sample has three points (three key features), and each summary plot contains 150,000 (structure I), 75,000 (structure II), and 75,000 (structure III) total points. Points with high feature values are colored in red while points with low feature values are colored in blue. For a given feature, different samples can have the same SHAP value, leading to the vertical clustering of points along the y-axis direction of the summary plots. The SHAP value of a point determines the contribution of the feature to the difference between the actual prediction for that sample and the classifier prediction. Positive SHAP values mean that the increase of feature values will lead to the selection of extraction. This allows us to understand how an increase in a feature value is likely to influence extraction feasibility and the selection between extraction and distillation.

We further use SHAP values to study how key features influence the prediction of classifiers. We identify $\alpha_{W,P}$ as the most important feature for all separation selection classifiers. We also observe that low $\alpha_{W,P}$ and low π^{EP} lead to extraction selection, while low κ_S leads to distillation selection, which are consistent with engineering experience. Specifically, low $\alpha_{W,P}$ leads to expensive distillation due to the large vapor flow, and thus energy consumption, in DIS. Also, low κ_S means that the solvent strongly partitions into the aqueous phase, resulting in high solvent loss, while π^{EP} has a direct influence on the extraction operating cost.

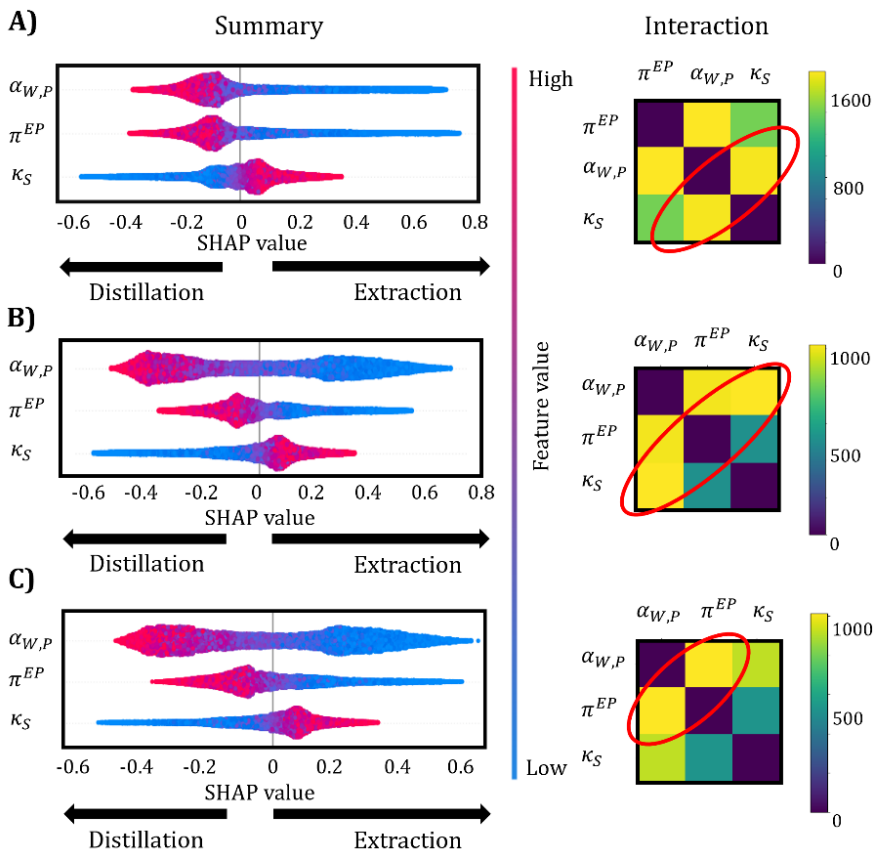

Figure 3. Interpretation of separation selection classifiers. A) structure I vs. distillation. B) structure II vs. distillation. C) structure III vs. distillation. Left panels show features' SHAP values. Right panels show pairwise feature interactions.

For each classifier, high values of pairwise feature interactions mean this pair of features has strong influence on the prediction of a classifier. Specifically, the Interaction plots of Figure S7 shows that the $\alpha_{W,P} - \alpha_{S,P}$ and $\tau - \kappa_P$ interactions have strong influence on the feasibility of structure I and structure III, respectively. The Interaction plots in Figure 3 show that the following interactions are important: $\alpha_{W,P} - \kappa_S$ and $\alpha_{W,P} - \pi^{EP}$ for structure I; $\alpha_{W,P} - \kappa_S$ for structure II; and $\alpha_{W,P} - \pi^{EP}$ for structure III. We further analyze them in the next two sections.

4.3. Extraction Feasibility

Among all pairwise feature interactions, the $\alpha_{W,P} - \alpha_{S,P}$ and $\tau - \kappa_P$ interactions have the strongest influence on the feasibility of structure I and structure III, respectively (see Figure S7 of the Supporting Information for details). For our analysis, we fix the values of the remaining features as follows. For structure I, we set: $\tau = 0.05$, to represent an intermediate product concentration; $\kappa_P = 5$, $\kappa_W = 0.01$, and $\kappa_S = 800$, to represent a solvent with mild product

partitioning into the SO phase and with high immiscibility with water; and $\pi^{EP} = \$2000$ per kmol solvent to represent an intermediate solvent price. For structure III, we set: $\alpha_{P,S} = 1.1$ and $\alpha_{W,S} = 1.21$, which means $\alpha_{W,P} = \alpha_{W,S}/\alpha_{P,S} = 1.21/1.1 = 1.1$ (see Section 2); $\kappa_W = 0.01$ and $\kappa_S = 800$; and $\pi^{EP} = \$5000$ per kmol solvent to represent an expensive solvent.

Figure 4A shows the cost of structure I for $\alpha_{W,P} \in [1.1, 2]$ and $\alpha_{S,P} \in [1.1, 2]$. Structure I appears infeasible around the $\alpha_{S,P} = \alpha_{W,P}$ line because 100 distillation stages are not enough to carry out the required separation. The water mole fraction in the extract stream is less than 1%, indicating that most water remains in the aqueous phase. The cost when $\alpha_{S,P} > \alpha_{W,P}$ (top-left region) is mostly lower than the cost when $\alpha_{S,P} < \alpha_{W,P}$ (bottom-right region). This is because introducing a more volatile solvent leads to an easier product-solvent separation than the product-water separation, while water from the initial feed remains in the raffinate stream of EXT. Moreover, in the top-left region, the cost of structure I tends to increase when both $\alpha_{S,P}$ and $\alpha_{W,P}$ decrease until 1.1, since the energy consumption for DIS increases significantly. In the bottom-right region, the cost of structure I tends to increase when $\alpha_{S,P}$ decreases because water is more volatile than the product and solvent and lower $\alpha_{S,P}$ means that more solvent exists at the bottom of DIS1. If the separation of product from solvent is difficult in DIS2 (i.e., under low $\alpha_{S,P}$), then the cost is high (bottom region of Figure 4A).

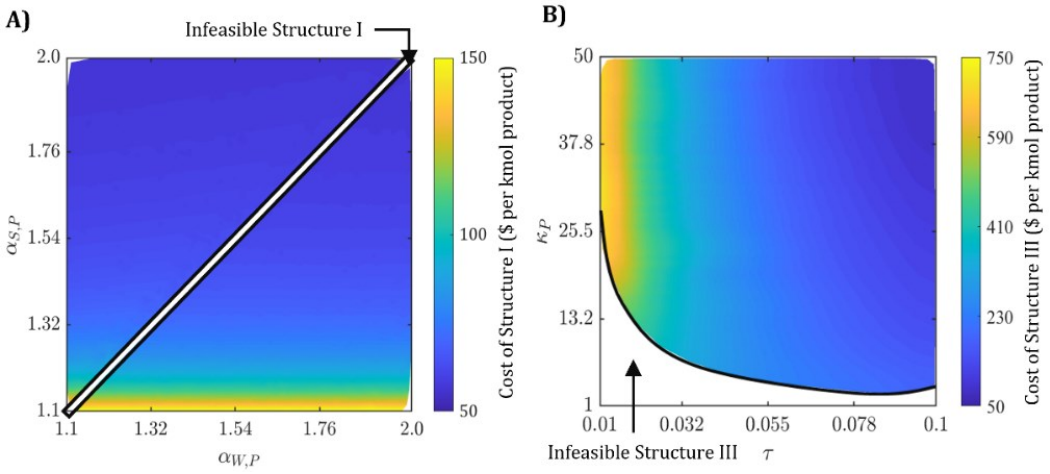

Figure 4. Influence of feature values on the cost of structure I (A) and structure III (B).

Figure 4B shows the cost of structure III when $\tau \in [0.01, 0.1]$ and $\kappa_P \in [1, 50]$. We observe that the system is infeasible (with an upper bound of 100 distillation stages) at low τ and low κ_P, and that the cost decreases as τ and κ_P increase. The width of the infeasible region tends to decrease when τ increases. This indicates that increasing τ can screen a solvent with

lower product partitioning capability (indicated by lower κ_P) to ensure that the separation design target can be achieved using structure III.

4.4. Selection between Extraction and Distillation

We further analyze the interactions shown to be important, in terms of separation technology selection, in Figure 3: $\alpha_{W,P} - \kappa_S$ and $\alpha_{W,P} - \pi^{EP}$. For both structure I and III, we investigate a third feature. As discussed in Section 4.1, π^{EP} is a key feature for structure I and hence we investigate its influence on the selection between structure I and distillation. We also investigate the influence of κ_S on the selection between structure III and distillation. The values of the remaining features are fixed as follows. For structure I, we set $\tau = 0.05$; $\alpha_{S,P} = 1.5$ to represent cases where water is lighter than solvent ($\alpha_{W,P} > 1.5 = \alpha_{S,P}$) or heavier than solvent ($\alpha_{W,P} < 1.5 = \alpha_{S,P}$); κ_P = 5 and $\kappa_W = 0.01$ to represent mild product partitioning into the solvent-rich phase and high immiscibility between solvent and water; and π^{EP} to three representative values (500, 2000, and \$5000/kmol). For structure III, we set $\tau = 0.05$ and $\alpha_{P,S} = 1.2$. As mentioned in Section 2.2, we convert $\alpha_{W,S}$ into $\alpha_{W,P}$ by dividing by $\alpha_{P,S}$. Since $\alpha_{W,S} \in [1.1, 2]$ and $\alpha_{W,S} > \alpha_{P,S}$, then $\alpha_{W,P} = (\frac{\alpha_{W,S}}{\alpha_{P,S}}) \in [1, 1.67]$. We set $\kappa_P = 5$ and $\kappa_W = 0.01$, and select κ_S at low (100), intermediate (500), and high (1000) values.

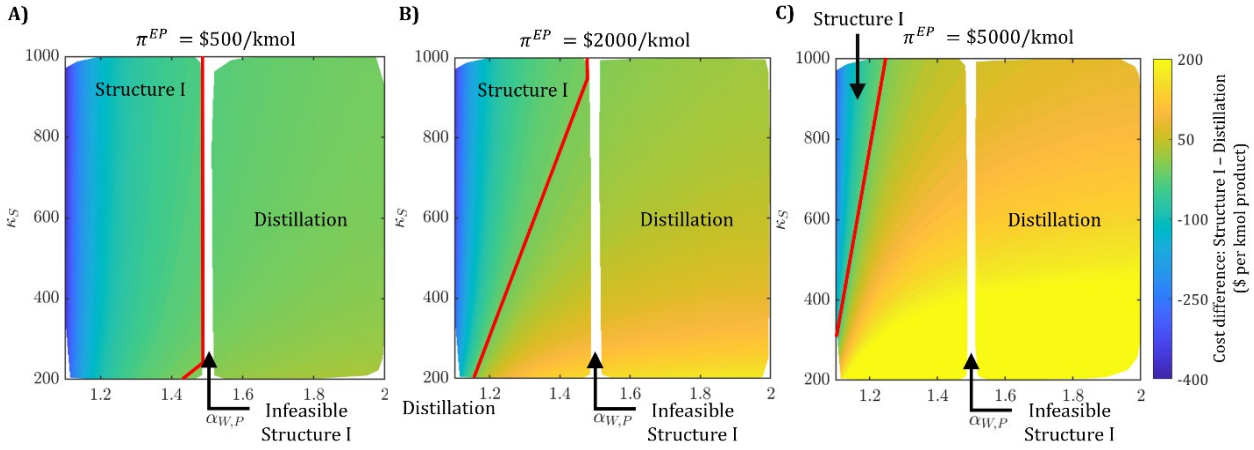

Figure 5. Influence of feature values on the cost difference between structure I and distillation at π^{EP}= \$500 per kmol solvent (A), π^{EP}= \$2000 per kmol solvent (B), and π^{EP}= \$5000 per kmol solvent (C). Structure I is selected on the left of red boundaries.

Figure 5 (structure I) and Figure 6 (structure III) show the feature influence on the cost difference between extraction and distillation. The difference is negative when the extraction

cost is lower than the cost of distillation. In all panels of Figure 5, extraction is infeasible at around $\alpha_{W,P} = 1.5$ because of the difficulty of solvent-water separation since $\alpha_{S,P} = 1.5$. Low $\alpha_{W,P}$ increases the cost of distillation. High κ_S leads to low solvent loss and thus low extraction operating cost. Hence, cost difference between structure I and distillation increase at low κ_S and high $\alpha_{W,P}$. As π^{EP} increases, the region where extraction is selected is reduced.

In Figure 6, since higher π^{EP} leads to higher extraction operating cost and higher $\alpha_{W,P}$ results in an easier distillation, the cost difference between structure III and distillation significantly increases when π^{EP} and $\alpha_{W,P}$ increase. Moreover, with the increase of κ_S, the region where structure III is selected is expanded. This is because the solvent loss decreases. When $\kappa_S = 1000$, for an easy distillation of product and water ($\alpha_{W,P} = 1.67$), a solvent with $\pi^{EP} \leq \$500$ per kmol solvent can lead to a more economical structure III. This is because EXT leads to a higher product mole fraction in the feed of DIS1 (from 5% to 21.4%) although product partitioning into the SO phase is low at each extraction stage ($\kappa_P = 5$).

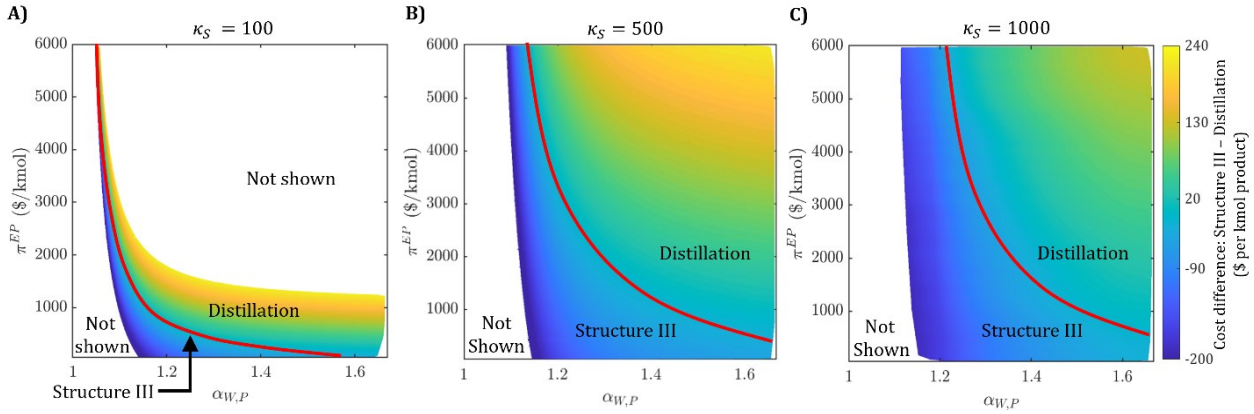

Figure 6. Influence of feature on the cost difference between structure III and distillation. A) At $\kappa_S = 100$. B) At $\kappa_S = 500$. C) At $\kappa_S = 1000$. Structure III is selected on the left of red boundaries.

4.5. Determination of Extraction Suitability

To facilitate the determination of the extraction suitability, we further train SVM based on the same initial training and test sets used for training RF. The trained SVM can be described using the explicit expression shown in Equation (3) to divide the feature space into regions where (1) extraction is infeasible, (2) extraction is selected, and (3) distillation is selected. For the extraction feasibility, the prediction accuracy of SVM for structure I and III are 0.98 and 0.98, respectively. For the selection between extraction and distillation, the prediction accuracy of SVM for structure I and III are 0.97 and 0.98, respectively. The hyperparameters for these

expressions are given in Section S6 of Supporting Information. To illustrate the use of these explicit expressions, we use an example of separating acetic acid (P) from water (W). Note that the boiling points of acetic acid and water are 391.2 K and 373.2 K, respectively.[43] We select this example system for the following reasons: (1) acetic acid is a common bioproduct produced in aqueous phase,[44] (2) the mixture of acetic acid and water is a close-boiling mixture, which makes distillation expensive, (3) the corresponding thermodynamic properties are within the investigated ranges of feature values, and (4) the separation of acetic acid from water is an industrially relevant example.[45] We consider $\tau = 0.05$ and we determine $\alpha_{W,P} = 1.32$ using the procedure described in the Supporting Information (Section S6). We consider structure III. We investigate the influence of interaction $\alpha_{S,P} - \kappa_P$ on the extraction suitability ($\alpha_{S,P}$ is related with DIS and κ_P is related with EXT). Since $\alpha_{W,S}$ is within [1.1, 2], $\alpha_{P,S} \geq 1.1$, and $\alpha_{P,S} = \frac{\alpha_{W,S}}{\alpha_{W,P}}$, $\alpha_{P,S}$ is within [1.1, 1.52]. When training classifiers, we use $\alpha_{S,P}$ as the input feature (determined as $\frac{1}{\alpha_{P,S}}$). Hence, $\alpha_{S,P}$ is within [0.66, 0.91]. At $\tau = 0.05$ and $\alpha_{W,P} = 1.32$, distillation cost is \$86.57 per kmol product. We set $\kappa_S = 1000$ (intermediate solvent loss), $\kappa_W = 0.01$ (low partitioning of water into the SO phase), and $\pi^{EP} = \$3000$ per kmol solvent (intermediate solvent price).

As shown in Figure 7, using the SVM-based explicit expressions, we identify the regions where structure III is infeasible, structure III is selected, and distillation is selected. We first generate 2000 values of feature vectors using Latin Hypercube sample (Figure 7A). Next, by applying the extraction feasibility classifier, we predict extraction feasibility (shown in Figure 7B). Using the separation selection classifier, we consider the region where structure III is feasible and classify points based on the preferred technology. The boundaries of different regions in Figure 7B (feasibility of structure III) and Figure 7C (structure III or distillation) are merged in Figure 7D. Figure 7D shows that the region defined by $\alpha_{S,P} \in [0.66, 0.91]$ and $\kappa_P \in [1, 50]$ is divided into three subregions, identified using the SVM-based explicit expressions within 1 CPU minute.

The direct optimization using models for extraction and distillation gives similar regions (Figure S8). At low κ_P (below grey boundary in Figure 7D), we observe the region where extraction is infeasible due to low partitioning of product into the extract stream. At higher $\alpha_{S,P}$, mole fractions of solvent and acetic acid are higher at the bottom of DIS1. When $\alpha_{S,P}$ (or $\alpha_{P,S}$) is approaching 0.91 (or 1.1), the separation of product from solvent at DIS2 is more difficult. This suggests that structure III is selected on the left of the black boundary. Moreover, the region

where extraction is selected is expanded with increasing κ_P because mole fraction of acetic acid is higher in the extract stream, which increases the acetic acid mole fraction in the feed of DIS1 and reduces distillation operating cost.

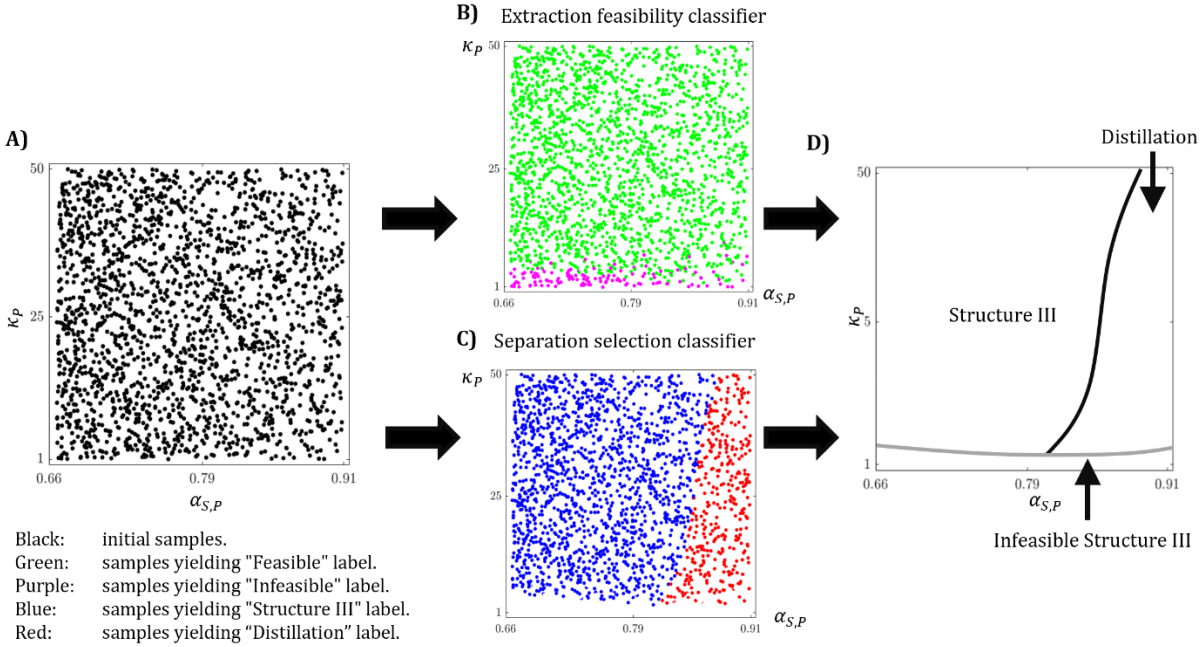

Figure 7. Analysis for separation of acetic acid from water. A) Initial samples. B) Extraction feasibility classifier. C) Separation selection classifier. D) Decision boundaries in feature space.

5. Conclusions

We proposed an explainable classification framework to, first, identify the key features that influence the suitability of extraction for the recovery of bioproducts from aqueous solutions; and, second, understand how these features quantitively determine when extraction (combined with distillation for solvent recovery) will be preferable over the standalone distillation, which is the separation method that is still broadly used in practice. We trained random forest classifiers to predict (1) extraction feasibility and (2) the suitability of extraction versus distillation. We showed that the key features are liquid-liquid equilibrium constants, relative volatilities, the product mole fraction in the feed, and the solvent price. We used Shapley values to interpret the influence of features on the prediction of the classifiers and, importantly, generate design guidelines. We performed sensitivity analysis in a subspace of key features to understand how they influence extraction feasibility, and the selection between extraction and distillation. We applied the proposed framework to a case study involving the recovery of acetic acid from water. Future work involves the development of a rapid screening tool for solvent

identification.

Acknowledgment

This material is based upon work supported by the Great Lakes Bioenergy Research Center, U.S. Department of Energy, Office of Science, Office of Biological and Environmental Research under Award Nos. DE-SC0018409. Jianping Li appreciates the Keegstra Fellowship awarded by the Great Lakes Bioenergy Research Center, U.S. Department of Energy.

Supporting Information

Nomenclature, parameter calculations, mathematical formulations for extraction and distillation systems, and additional result discussions.

References

1 Alonso, D. M.; Hakim, S. H.; Zhou, S.; Won, W.; Hosseinaei, O.; Tao, J.; Garcia-Negron, V.; Motagamwala, A. H.; Mellmer, M. A.; Huang, K. Increasing the revenue from lignocellulosic biomass: Maximizing feedstock utilization. *Sci. Adv.* **2017**, *3* (5), e1603301.

2 U.S. DOE. U.S. Department of Energy Bioenergy Research Centers, DOE/SC–0191. U.S. Department of Energy Office of Science (genomicscience.energy.gov/centers/brcbrochure.pdf). 2018.

3 Huang, K.; Peng, X.; Kong, L.; Wu, W.; Chen, Y.; Maravelias, C. T. Greenhouse gas emission mitigation potential of chemicals produced from biomass. *ACS Sustain. Chem. Eng.* **2021**, *9* (43), 14480-14487.

4 Luterbacher, J.; Alonso, D. M.; Dumesic, J. Targeted chemical upgrading of lignocellulosic biomass to platform molecules. *Green Chem.* **2014**, *16* (12), 4816-4838.

5 Velasco, J. A. C.; Tawarmalani, M.; Agrawal, R. Systematic analysis reveals thermal separations are not necessarily most energy intensive. *Joule.* **2021**, *5* (2), 330-343.

6 Seader, J. D.; Henley, E. J.; Roper, D. K. *Separation process principles*; wiley New York, 1998.

7 Ryu, J.; Maravelias, C. T. Computationally efficient optimization models for preliminary distillation column design and separation energy targeting. *Comput. Chem. Eng.* **2020**, *143*, 107072.

8 Li, J.; Demirel, S. E.; Hasan, M. M. F. Systematic Process Intensification involving Zeotropic Distillation. In *Comput. Aided Chem. Eng.* 47, **2019**, 421-426.

9 Weeranoppanant, N.; Adamo, A.; Saparbaiuly, G.; Rose, E.; Fleury, C.; Schenkel, B.; Jensen, K. F. Design of multistage counter-current liquid–liquid extraction for small-scale applications. *Ind. Eng. Chem. Res.* **2017**, *56* (14), 4095-4103.

10 Blahušiak, M.; Kiss, A. A.; Kersten, S. R.; Schuur, B. Quick assessment of binary distillation efficiency using a heat engine perspective. *Energy.* **2016**, *116*, 20-31.

11 Restrepo-Flórez, J. M.; Maravelias, C. T. Advanced fuels from ethanol–a superstructure optimization approach. *Energ Environ. Sci.* **2021**, *14* (1), 493-506.

12 Li, J.; Demirel, S. E.; Hasan, M. M. F. Process integration using block superstructure. *Ind. Eng. Chem. Res.* **2018**, *57* (12), 4377-4398.

13 Agrawal, R.; Tumbalam Gooty, R. Misconceptions about efficiency and maturity of distillation. *AIChE J.* **2020**, *66* (8), e16294.

14 Kiss, A. A.; Smith, R. Rethinking energy use in distillation processes for a more sustainable chemical

industry. *Energy.* **2020**, *203*, 117788.

15 Li, J.; Hasan, M. M. F. A parametric approach to identify synergistic domains of process intensification for reactive separation. *Chem. Eng. Sci.* **2023**, *267*, 118337.

16 Castillo-Landero, A.; Dominguillo-Ramirez, D.; Aburto, J.; Sadhukhan, J.; Martinez-Hernandez, E. Improving the Economic, Environmental, and Safety Performance of Bio-Jet Fuel Production through Process Intensification and Integration Using a Modularity Approach. *ACS Sustain. Chem. Eng.* **2023**, *11* (2), 660-669.

17 Hanson, C. Recent advances in liquid-liquid extraction. *Elsevier Science*. **2013**.

18 Nguyen, H.; DeJaco, R. F.; Mittal, N.; Siepmann, J. I.; Tsapatsis, M.; Snyder, M. A.; Fan, W.; Saha, B.; Vlachos, D. G. A review of biorefinery separations for bioproduct production via thermocatalytic processing. *Annu. Rev. Chem. Biomol. Eng.* **2017**, *8*, 115-137.

19 Perez, J. M.; Sener, C.; Misra, S.; Umana, G. E.; Coplien, J.; Haak, D.; Li, Y.; Maravelias, C. T.; Karlen, S. D.; Ralph, J. Integrating lignin depolymerization with microbial funneling processes using agronomically relevant feedstocks. *Green Chem.* **2022**, *24* (7), 2795-2811.

20 Taifan, G. S.; Maravelias, C. T. Integration of graphical approaches into optimization-based design of multistage liquid extraction. *Comput. Chem. Eng.* **2020**, *143*, 107126.

21 Eldridge, R. B.; Seibert, A. F.; Robinson, S.; Rogers, J. Hybrid separations/distillation technology. Research opportunities for energy and emissions reduction. Industrial Technologies Program, U.S. Department of Energy. **2005**.

22 Kraemer, K.; Harwardt, A.; Bronneberg, R.; Marquardt, W. Separation of butanol from acetone–butanol–ethanol fermentation by a hybrid extraction–distillation process. *Comput. Chem. Eng.* **2011**, 35 (5), 949-963.

23 Harvianto, G. R.; Kang, K. J.; Lee, M. Process design and optimization of an acetic acid recovery system in terephthalic acid production via hybrid extraction–distillation using a novel mixed solvent. *Ind. Eng. Chem. Res.* **2017**, 56 (8), 2168-2176.

24 Nhien, L. C.; Long, N. V. D.; Kim, S.; Lee, M. Techno-economic assessment of hybrid extraction and distillation processes for furfural production from lignocellulosic biomass. *Biotechnol. Biofuels.* **2017**, *10* (1), 1-12.

25 Scheffczyk, J.; Schäfer, P.; Fleitmann, L.; Thien, J.; Redepenning, C.; Leonhard, K.; Marquardt, W.; Bardow, A. COSMO-CAMPD: a framework for integrated design of molecules and processes based on COSMO-RS. *Mol. Syst. Des. Eng.* **2018**, *3* (4), 645-657.

26 Blahušiak, M.; Kiss, A. A.; Babic, K.; Kersten, S. R.; Bargeman, G.; Schuur, B. Insights into the selection and design of fluid separation processes. *Sep. Purif. Technol.* **2018**, *194*, 301-318.

27 Ryu, J.; Maravelias, C. T. Efficient generalized shortcut distillation model with improved accuracy for superstructure-based process synthesis. *AIChE J.* **2020**, *66* (11), e16994.

28 Kiss, A. A.; Lange, J.-P.; Schuur, B.; Brilman, D. W. F.; van der Ham, A. G.; Kersten, S. R. Separation technology–Making a difference in biorefineries. *Biomass Bioenergy.* **2016**, *95*, 296-309.

29 Breiman, L. Random forests. *Machine learning* **2001**, *45* (1), 5-32.

30 Pedregosa, F.; Varoquaux, G.; Gramfort, A.; Michel, V.; Thirion, B.; Grisel, O.; Blondel, M.; Prettenhofer, P.; Weiss, R.; Dubourg, V. Scikit-learn: Machine learning in Python. *J. Mach. Learn. Res.* **2011,** 12, 2825-2830.

31 Campbell, C.; Ying, Y. Learning with support vector machines. *Synth. Lect. Artif. Intell. Mach. Learn.* **2011**, *5* (1), 1-95.

32 Zhai, J.; Boukouvala, F. Nonlinear variable selection algorithms for surrogate modeling. *AIChE J.* **2019**, *65* (8), e16601.

33 Chang, C.-C.; Lin, C.-J. LIBSVM: a library for support vector machines. *ACM Trans. Intell. Syst. Technol.* **2011**, *2* (3), 1-27.

34 Shapley, L. Quota Solutions Op N-Person Games1. Contributions to the Theory of Games, Volume II, **1953**, 343.

35 Zamir, S.; Maschler, M.; Solan, E. *Game theory*; Cambridge University Press, **2020**.

36 Lundberg, S. M.; Lee, S.-I. A unified approach to interpreting model predictions. *Adv. Neural Inf. Process. Syst.* **2017**, *30*, 1.

37 Lundberg, S. M.; Erion, G.; Chen, H.; DeGrave, A.; Prutkin, J. M.; Nair, B.; Katz, R.; Himmelfarb, J.; Bansal, N.; Lee, S.-I. From local explanations to global understanding with explainable AI for trees. *Nat. Mach. Intell.* **2020**, *2* (1), 56-67.

38 Li, J.; Maravelias, C. T.; Van Lehn, R. C. Adaptive Conformer Sampling for Property Prediction Using the Conductor-like Screening Model for Real Solvents. *Ind. Eng. Chem. Res.* **2022**, *61* (25), 9025-9036.

39 Qin, S.; Jiang, S.; Li, J.; Balaprakash, P.; Van Lehn, R. C.; Zavala, V. M. Capturing molecular interactions in graph neural networks: a case study in multi-component phase equilibrium. *Digit. Discov.* **2023**, *2* (1), 138-151.

40 Sahinidis, N. V.; Tawarmalani, M. BARON 7.2. 5: Global optimization of mixed-integer nonlinear programs. *User's manual* **2005**.

41 Palach, J. *Parallel programming with Python*; Packt Publishing Ltd, 2014.

42 Hunt, B. R.; Lipsman, R. L.; Rosenberg, J. M. *A guide to MATLAB: for beginners and experienced users*; Cambridge university press, **2014**.

43 Lemmon, E. W.; Huber, M. L.; McLinden, M. O. NIST standard reference database 23. *Reference fluid thermodynamic and transport properties (REFPROP), version* **2010**, *9*.

44 Ijmker, H.; Gramblička, M.; Kersten, S. R.; van der Ham, A. G.; Schuur, B. Acetic acid extraction from aqueous solutions using fatty acids. *Sep. Purif. Technol.* **2014**, *125*, 256-263.

45 García, N.; Caballero, J. A. Economic and environmental assessment of alternatives to the extraction of acetic acid from water. *Ind. Eng. Chem. Res.* **2011**, *50* (18), 10717-10729.

Synopsis

We develop an explainable classification framework to analyze and understand the use of combined extraction and distillation for bioproduct recovery.
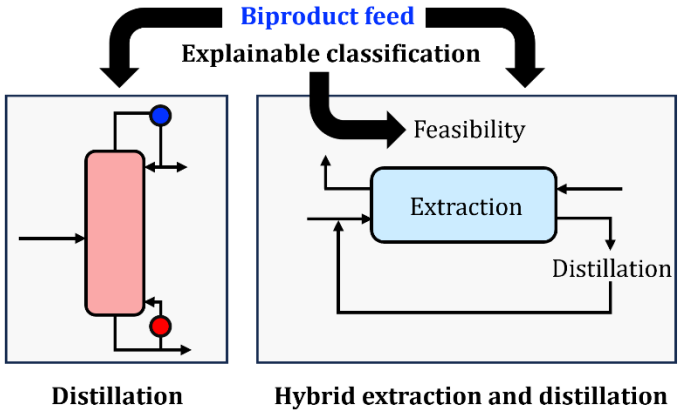
TOC Graphic